New Planar and Volume Versions of a Metamaterial

Jan MACHÁČ, Martin HUDLIČKA, Pavel BUCHAR, Ján ZEHENTHER

Dept. of Electromagnetic Field, Czech Technical University, Technická 2, 166 27 Praha 6, Czech Republic

machac@fel.cvut.cz, hudlicm@fel.cvut.cz, bucharp@fel.cvut.cz, zehent@fel.cvut.cz

Abstract. *Some characteristics of materials with negative permittivity and permeability, i.e., with a negative refractive index, known as metamaterials, are presented in this paper. Dispersion characteristics of left-handed parallel strips calculated by different methods are compared with each other. The calculated and measured dispersion and transmission characteristics of a newly proposed left-handed coplanar waveguide and of a novel volume metamaterial are shown. Simple equivalent circuits of both structures are presented together with elements values. The structures exhibit a negative refractive index in a wide frequency band.*

Keywords

Periodic structure, metamaterial, coplanar waveguide, dispersion characteristic, Floquet's theorem.

1. Introduction

Unlike standard natural materials having positive values of permittivity and permeability, i.e., positive refractive index, metamaterials may exhibit both positive and negative values. This fact opens huge opportunities for various applications [1]-[3]. In this way, media with negative permittivity and permeability can be obtained. Metamaterials are also called left-handed (LH) materials, according to the orientation of the vectors of the electric and magnetic field with a propagating vector of a traveling wave. The unique properties of these materials may have practical applications, e.g., as antennas [4], phase shifters [5], hybrid ring couplers [6], ideal lenses [7], single mode waveguides [8], zeroth order resonators [9], perfect magnetic layers [10], etc. Inclusions as lumped elements imply more complex fabrication, and for this reason planar structures have mostly received considerable attention [11], [12], [13].

LH transmission lines and materials are structures with periodically inserted inclusions. If the dimensions of an inclusion, i.e., a cell of this periodic structure, are infinitesimal, then this medium can be treated as continuous. Otherwise the medium must be treated as a periodic structure and the dispersion characteristic is determined by the use of the Floquet's theorem. The dispersion characteristic can also be calculated numerically using a full-wave elec-

tromagnetic field solver, e.g., CST Microwave Studio (MwS). The application of these methods is documented on LH parallel strips.

In the paper a new LH coplanar waveguide (LHCPW) is presented along with a new bulk metamaterial. These structures follow the concept of the LH parallel strips described in the paper and show LH behavior in a wide frequency band. The metamaterials were manufactured and measured. The calculated characteristics fit the measured data well. In this paper, the volume, or bulk, metamaterial is understood as a material, which on contrary to a planar transmission line, occupies some volume and is aimed at volume applications. It is excited by a plane electromagnetic wave with the given polarization and the direction of propagation. Hence this metamaterial is non-isotropic.

2. Concept of an LH Medium and Its Dispersion Characteristic

Media transmitting an electromagnetic wave can be modeled by an equivalent homogeneous transmission lines. The circuit model of one elementary cell of these lines is shown in Fig. 1a. It consists of series impedance Z_s and parallel admittance Y_p. These values Z_s and Y_p are taken per unit length. The length d of this cell is infinitesimally short. The characteristic impedance Z_0 and the propagation constant $\gamma = \alpha - \mathrm{j}\beta$ of this transmission line are [14]
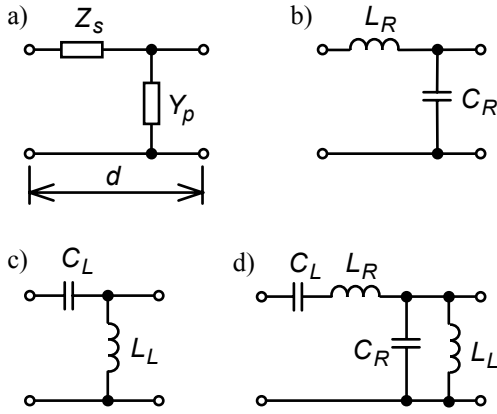
$$Z_0 = \sqrt{\frac{Z_s}{Y_p}} \ , \tag{1}$$

$$\gamma = \pm\sqrt{Z_s Y_p} \ . \tag{2}$$

For a standard transmission line the series impedance is inductive and represents the stored energy of the magnetic field. The shunt admittance is capacitive and represents the stored energy of the electric field, Fig. 1b. Thus for a lossless line we have $Z_s = \mathrm{j}\omega L_R$, $Y_p = \mathrm{j}\omega C_R$, and the well known formulas follow from (1), (2)

$$Z_0 = \sqrt{\frac{L_R}{C_R}} \ , \tag{3}$$

$$\gamma = \mathrm{j}\beta = \mathrm{j}\omega\sqrt{L_R C_R} \ . \tag{4}$$

Fig. 1. The equivalent circuit of a general transmission line (a), a standard L-C line (b), a C-L left-handed line (c), and a real LH transmission line (d). All circuit elements are taken per unit length.

From (4) we obtain phase velocity equal to group velocity. This γ (4) corresponds to propagation of a standard forward wave along the line known as a right-handed (RH) wave.

Let us now consider the dual case with exchanged positions of the capacitor and the inductor, Fig. 1c. We have changed the original L-C low-pass structure to a C-L high-pass structure. For a lossless line $Z_s = 1/(j\omega C_l)$ and $Y_p = 1/(j\omega L_L)$. Inserting them into (1), (2) we get

$$Z_0 = \sqrt{\frac{L_L}{C_L}} \ , \tag{5}$$

$$\beta = -\frac{1}{\omega\sqrt{L_L C_L}} \ . \tag{6}$$

Subsequently, we obtain values of phase and group velocities from the phase constant (6)

$$v_p = \frac{\omega}{\beta} = -\omega^2 \sqrt{L_L C_L} \ , \tag{7}$$

$$v_g = \frac{\partial \omega}{\partial \beta} = \omega^2 \sqrt{L_L C_L} \ . \tag{8}$$

Different signs in (7) and (8) may be observed. The group velocity has the opposite direction to the phase velocity. This is a feature of a backward wave known as a left-handed wave. The phase changes in the direction opposite to the flow of the transmitted power. The magnitude of the phase constant decreases with frequency, which means that the wavelength increases with frequency.

An LH transmission line having the equivalent circuit from Fig. 1c cannot be fabricated as simply as we have introduced. The inductors and capacitors are inserted into a real hosting environment, which has the character shown in Fig. 1b. Therefore combining the circuits from Figs. 1b, c we get the cell equivalent circuit as shown in Fig. 1d. The series impedance, the parallel admittance and the phase constant are

$$Z_s = j\omega L_R + \frac{1}{j\omega C_L} \ , \tag{9}$$

$$Y_p = j\omega C_R + \frac{1}{j\omega L_L} \ , \tag{10}$$

$$\beta = \sqrt{\omega^2 L_R C_R + \frac{1}{\omega^2 L_L C_L} - \left(\frac{L_R}{L_L} + \frac{C_R}{L_L}\right)} \ . \tag{11}$$

Eqn. (11) is valid only when the cell length is infinitesimal. If this is not the case and the cell length is comparable to the wavelength, the line must be treated as a periodic structure. To derive the dispersion characteristic of a periodic structure the transmission matrix of the cell is calculated according to [15]. Applying Floquet's theorem [15] we get

$$\cos(\beta d) = \cos(kd) - \frac{d^2}{2\omega^2 L_L C_L} \cos^2\left(\frac{kd}{2}\right) + $$
$$+ \frac{d}{2}\sin(kd)\left(\frac{1}{\omega C_L Z_0} + \frac{Z_0}{\omega L_L}\right). \tag{12}$$

The dispersion characteristic of an arbitrary transmission line can be calculated by MwS in the following way [16]. The elementary cell of the line is terminated at input and output faces by periodical boundaries with varying mutual phase shift φ. The resonant frequencies of this cell, which represents now a resonator, are calculated by the MwS eigenmode solver in dependence on φ. This phase shift determines the phase constant

$$\beta = \varphi/d \ . \tag{13}$$

The calculated resonant frequency represents the second variable of the dispersion relation.

3. LH Parallel Strips

We document the behavior of an LH transmission line on parallel strips. This line is shown in Fig. 2. One of the strips is periodically cut by slots representing the series capacitors, and the line is loaded by shunt pins representing the parallel inductors. On its sides the line is terminated by perfect magnetic walls. The dielectric between the strips has permittivity $\varepsilon_r = 2.6$, is $t = 2$ mm in thickness and $w = 10$ mm in width. The length of one cell is $d = 4$ mm, the slot width is 0.05 mm and the diameter of the inductive pins is 0.2 mm. The parameters of the hosting line are calculated from (3) and (4). Assuming [14]

$$Z_0 = \sqrt{\frac{\mu_0}{\varepsilon_0 \varepsilon_r}}\frac{t}{w}, \quad \beta = \frac{\omega}{c}\sqrt{\varepsilon_r} \ , \tag{14}$$

we get $L_R = 1.02$ nH, $C_R = 0.47$ pF. The values L_L and C_L can be calculated from zeros of the phase constant (11) which coincidences with the edges of the stop-band calculated by the MwS, Fig. 3. This gives $C_L = 1.38$ pF and $L_L = 1.4$ nH.

The dispersion characteristics of the LH parallel strips computed by MwS, calculated as a periodic structure by (12) and calculated as a homogeneous transmission line by (11), are compared in Fig. 3. At low values of the phase constant these three characteristics are nearly identical. At higher values of β the length of the cell is not negligibly short compared to the wavelength, and the line model (11) is not valid.
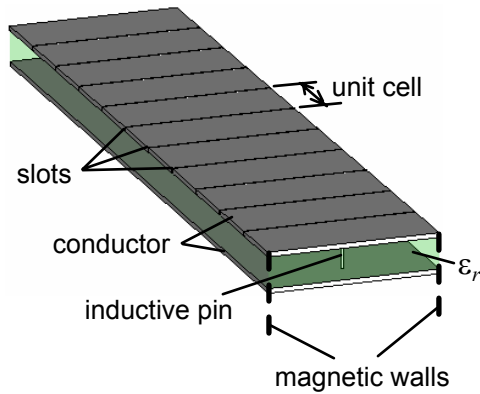

Fig. 2. LH parallel strips.

Two lowest pass-bands of the line are shown in Fig. 3. The LH wave propagates in the first band from about 2 GHz to 4 GHz. The standard RH wave propagates in the second pass-band from about 6 to 23 GHz. There is a stop-band between these two pass-bands and a stop-band below the LH pass-band due to the high-pass character of the line.
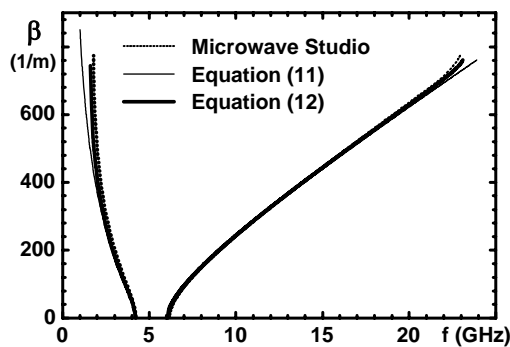

Fig. 3. The dispersion characteristics of the LH parallel strips from Fig. 2 calculated by the CST Microwave Studio, and by (11) and (12).

4. LH Coplanar Waveguide

The structure of the LHCPW does not contain any lumped elements. Its layout is a modification of the line described in [11], but is more compact. The line presented here is applied in microwave circuits, whereas the structure in [11] was aimed for a leaky wave antenna design. One half of the layout of the LHCPW, Fig. 4, fulfills the notion of an ideal LH transmission line, Fig. 1c. The series capacitor is represented by an interdigital capacitor, and the parallel inductor creates the input impedance of the short-circuited CPW stubs connected to the ground metallization.

These elements are frequency dependent and the equivalent circuit of the cell is more complicated, as parasitic elements and the hosting CPW must be taken into account. By periodical translation of the unit cell we get the layout of the LHCPW shown in Fig. 5. The dispersion characteristics of the waves propagating along the LHCPW calculated by MwS are plotted in Fig. 6. Each branch of the dispersion characteristic in Fig. 6 defines one pass-band. In the first and third pass-bands the LH wave propagates, the phase constant decreases and the wavelength increases with frequency. In the second and fourth pass-bands the RH wave propagates, and the phase constant increases with frequency. In this paper, we focus on the first pass-band.
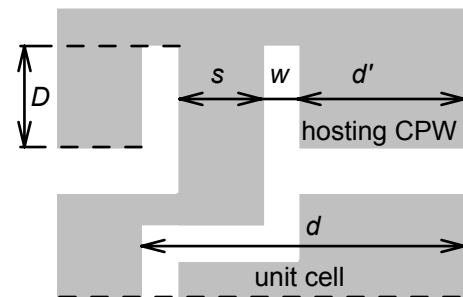

Fig. 4. One half of the unit cell of the LHCPW.

Fig. 7 compares the first branch of the dispersion characteristic from Fig. 6 with the measured phase constant and with the phase constant computed using an equivalent circuit described below. The LH wave propagates from 5.1 to 6.4 GHz, as shown in Figs. 6 and 7, but the practical transmission band is narrower, as follows from the transmission characteristic of the line.
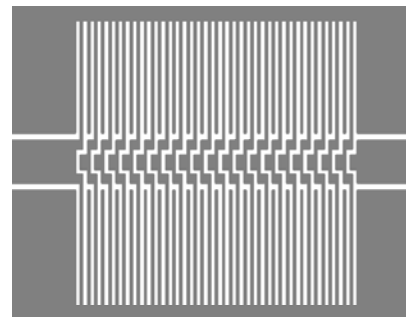

Fig. 5. Final layout of the LHCPW.

The usable frequency band is about 13% of the central frequency. The modulus of S_{21} computed by MwS is compared with the measured modulus in Fig. 8. Both curves fit well in frequency band the first LH mode propagates.

4.1 Equivalent Circuit of the LHCPW

The equivalent circuit of the unit cell of the LHCPW is shown in Fig. 9. This circuit contains 4 unknowns (2 inductors and 2 capacitors) and is able to approximate the dispersion characteristic of the first left-handed mode very accurately. It consists of L_R, C_R elements representing the hosting CPW with the characteristic impedance (3) and the propagation constant (4), denoted here as k. The impedance

Z_{in} represents the input impedance of a short-circuited CPW with finite-extent ground planes of length D, which is given by the relation

$$Z_{in} = jZ_{0e} \tan(\beta_0 D)/2 \ , \tag{15}$$

where Z_{0e} is characteristic impedance of even mode of the CPW with finite-extent ground planes [17], and β_0 is phase constant of this line. In our case, the stub length is $D=7$ mm and $Z_{0e}=148.6 \ \Omega$ and Z_{in} shows the inductive behavior.
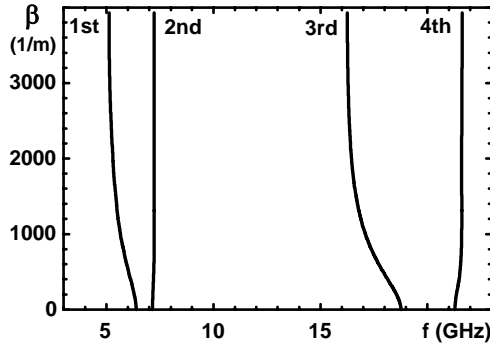

Fig. 6. Dispersion characteristics of the four lowest modes on the LHCPW from Fig. 4.
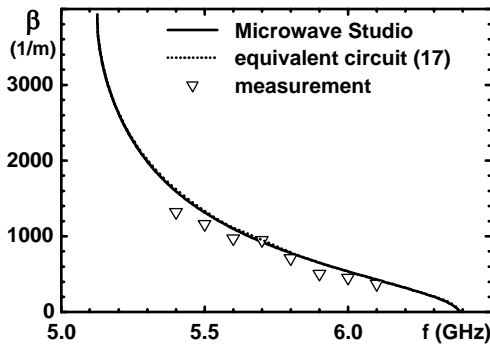

Fig. 7. Calculated and measured dispersion characteristic of the LHCPW from Fig. 5.
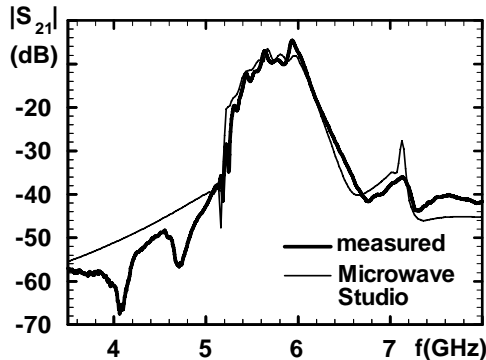

Fig. 8. Measured and calculated modulus of S_{21} of the manufactured LHCPW.

An ideal left-handed transmission line consists only of series capacitor C_1 and the parallel inductor formed by the impedance Z_{in}. Parasitic series inductor L_2 and parallel capacitor C_2 have been added to the model of the LHCPW

layout to make it more realistic. This circuit satisfactorily models the interdigital capacitor and the parallel short-circuited CPW stubs. The effect of the coupling between neighbouring cells is not taken into account. The equivalent circuit is proposed to model only the dispersion characteristic of the first left-handed mode.
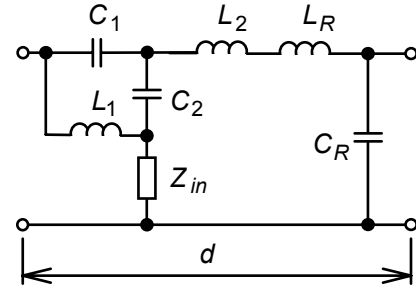

Fig. 9. Equivalent circuit of the unit cell in Fig. 4.
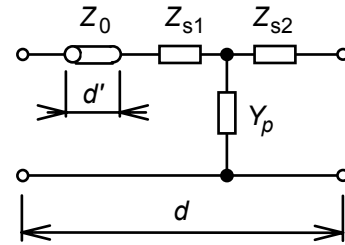

Fig. 10. Modification of the equivalent circuit in Fig. 9 for derivation of the dispersion characteristic.

The dispersion characteristic is derived using the modified equivalent circuit shown in Fig. 10, where L_R, C_R are replaced by a section of the transmission line with characteristic impedance Z_0, phase constant k and length d'. The length of the whole unit cell is d, see Fig. 4. The ABCD matrix of the unit cell is calculated [15]. Then the dispersion characteristic is obtained by applying Floquet's theorem in the form

$$\cos(\beta d) = \frac{1}{2}\left(2 + Y_p(Z_{s1} + Z_{s2})\right)\cos(kd') + $$
$$+ \frac{j}{2Z_0}\left(Z_{s1} + Z_{s2} + Y_p(Z_0^2 + Z_{s1}Z_{s2})\right)\sin(kd') \ , \tag{16}$$

where

$$Z_{s1} = \frac{L_1/C_1}{j\omega L_1 + 1/(j\omega C_1) + 1/(j\omega C_2)} \ , \tag{17}$$

$$Z_{s2} = \frac{-1/(\omega^2 C_1 C_2)}{j\omega L_1 + 1/(j\omega C_1) + 1/(j\omega C_2)} + j\omega L_2 \ , \tag{18}$$

$$Y_p = \left(\frac{L_1/C_2}{j\omega L_1 + 1/(j\omega C_1) + 1/(j\omega C_2)} + jZ_{0e}\tan(\beta_0 D)\right)^{-1} . \tag{19}$$

The circuit elements Z_{s1}, Z_{s2} and Y_p are obtained by the star-delta transformation of elements L_1, C_1, C_2 and by some additional circuit rearrangements.

A comparison of the dispersion characteristics computed by (16), measured and computed by the MwS, is shown in Fig. 7, where only the first LH mode is depicted. It can be seen that the curve calculated by (16) approximates the dispersion characteristic of the first LH mode very accurately. The values of the lumped elements from Fig. 9 were determined by fitting the dispersion characteristic defined by (16) to the dispersion characteristic calculated by MwS. The resulting values are L_1=99 nH, C_1=0.091 pF, L_2=7.25 nH and C_2=0.34 pF.
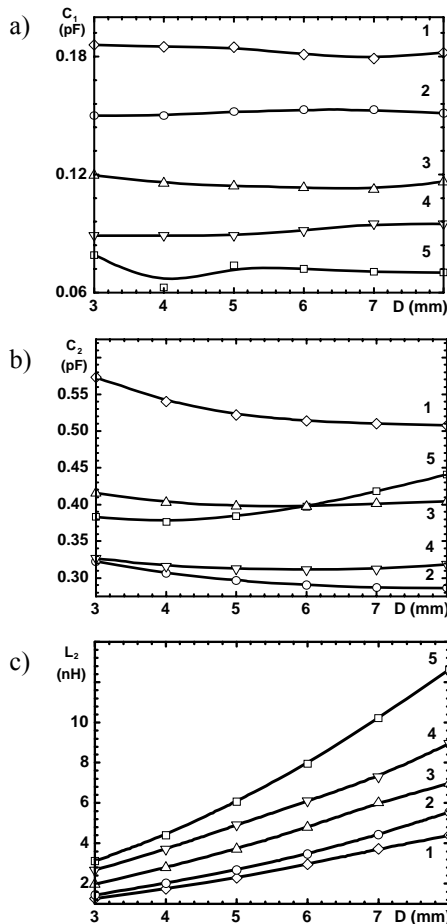
Fig. 11. Values C1 (a), C2 (b), and L2 (c) calculated for different D, s, and w. 1 – s=0.4 mm, w=0.1 mm, 2 – s=0.125 mm, w= =0.275 mm, 3 – s=0.125 mm, w=0.1 mm, 4 – s=0.25 mm, w= =0.25 mm, 5 – s=0.125 mm, w=0.5 mm.

A very similar LHCPW was presented in [18], where also the equivalent circuit of the unit cell was determined. The equivalent circuit structure is the same like in Fig. 1d, where additional series resistance and shunt conductance were added. These equivalent circuit elements were extracted simultaneously from S-parameters based on effective medium theory [19]. The circuit elements, however, are valid only for one fabricated line and any dependence on the structure geometrical dimensions is missing.

## 4.2 LHCPW Equivalent Circuit Elements

In order to determine the equivalent circuit element values, several structures with the same shape as in Fig. 4

were simulated by the MwS. Stub length D, stub central conductor width s and stub slot width w were varied, Fig. 4. The dispersion characteristics computed using (16) were fitted to the characteristics computed by MwS, and the resulting element values are summarized in Fig. 11. The simulations were fulfilled in the range D = 3÷8 mm, s = 0.125÷0.4 mm and w = 0.1÷0.5 mm for several combinations of these dimensions. Each combination of the geometrical dimensions determines a different frequency band in which the first LH mode propagates.

It can be seen from Fig. 11 that the values of C_1 are roughly constant, the values of C_2 decrease slowly with growing D. Element L_2 shows a linear dependence on stub length D, which determines the frequency band of the first LH mode on the line. The value of L_1 varies ±0.5 % of its nominal value for every combination of geometrical dimensions, therefore it is not shown in Fig. 11.

5. LH Volume Structure

The proposed novel volume structure is shown in Fig. 12, along with the orientation of the electromagnetic wave propagating between the layers of the structure. It consists of a periodically repeated unit cell, which is shown in Fig. 13. The unit cell is repeated 6x15 times in the horizontal plane in one and two half layers placed vertically. The structure is vertically terminated by electric walls, which are placed at the horizontal symmetry planes of the layers.
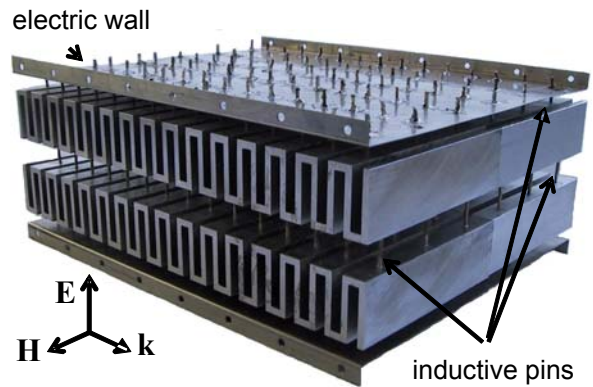
Fig. 12. Manufactured bulk metamaterial.

The idea of the structure also starts from the *L-C* equivalent circuit of Fig. 1c. The unit cell in Fig. 13 consists of a parallel-plate waveguide section, which is broken by serially connected vertical stubs and shunted by vertical pins. The vertical stubs are short-circuited. Their input impedance represents the series capacitance and the pins represent the shunt inductance. The dimensions of the structure were obtained by an optimization performed by the MwS with the aim to obtain a structure with a preferably wide frequency band of LH wave propagation, and at the same time to achieve the minimum of insertion losses. The structure was fabricated, measured and its equivalent circuit was determined.
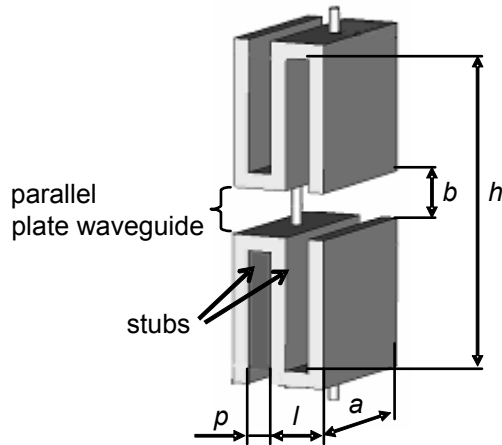
Fig. 13. Detail of one unit cell of the bulk material.

5.1 LH Volume Structure Equivalent Circuit

As has already been mentioned, the structure originates from the equivalent structure of Fig. 1c. A modified circuit suitable for deriving the dispersion relation is shown in Fig. 14. By applying Floquet's theorem, the dispersion relation was derived in the form

$$\cos(\beta d) = \cos(k_0 l') - \frac{1}{2\omega^2 LC}\cos^2\left(k_0\frac{l'}{2}\right) + $$
$$\frac{1}{2\omega}\left(\frac{1}{CZ_0} + \frac{1}{LY_0}\right)\sin(k_0 l'). \tag{20}$$

Here $d = p + l$ (Fig. 13) and $Z_0 = 1/Y_0$ is the impedance of the parallel-plate waveguide

$$Z_0 = \sqrt{\frac{\mu_0}{\varepsilon_0\varepsilon_r}}\frac{b}{a} \ , \tag{21}$$

where b is the thickness of the waveguide and a is its width. k_0 is the propagation constant of the electromagnetic wave propagating through the parallel-plate waveguide. C is the capacity at the input plane of the vertical stub. Its value is frequency dependent and may be obtained by the following formula

$$C = -\frac{1}{\omega\sqrt{\dfrac{\mu_0}{\varepsilon_0\varepsilon_r}}\dfrac{p}{a}\tan\left[\dfrac{\omega}{c_0}\sqrt{\varepsilon_r}\,(h-b)/2\right]} \ , \tag{22}$$

where p is the thickness of the stub and $(h-b)/2$ is its length, Fig. 13. L is the inductance of the pin, the value of which may be obtained using the formula [20]

$$L = 2\cdot10^{-7}\cdot b\left[\ln\left(\frac{b}{r\sqrt{\pi}}\right) + 0.5 + 0.447\frac{r\sqrt{\pi}}{b}\right], \tag{23}$$

where r is the radius of the pin. Finally, l' is the modified length of the parallel-plate waveguide section. Its real length has been increased in order to take into account scattering at the junction between the parallel plate waveguide and the vertical stub.
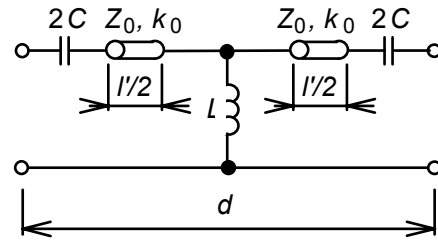

Fig. 14. Modified equivalent circuit of the unit cell in Fig 13.

In order to fit the dispersion characteristic obtained by MwS well, the real length was increased by empirically obtained 25%. The dispersion characteristic for our particular structure dimensions (a=20 mm, b=10 mm, h=24 mm, p=3 mm, r=0.5 mm, d=10 mm) and ε_r=1 is shown in Fig. 15 in comparison with the dispersion characteristic obtained by the MwS and with the dispersion characteristic obtained by measurement of the fabricated structure. It can be seen that characteristics obtained by the different methods fit each other quite well, mainly in the high wavelength limit area (for $\beta\rightarrow0$), where the transmission line equivalent circuit model may be correctly used.
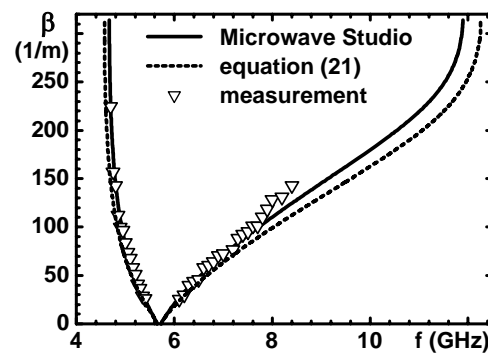

Fig. 15. The dispersion characteristic of the bulk structure.
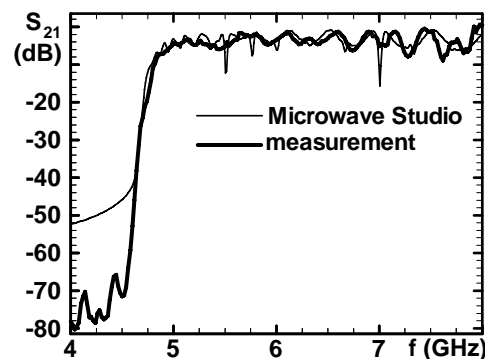

Fig. 16. S_{21} of the bulk structure.

The frequency dependence of the transmission coefficient of the structure (measured and calculated by the MwS) is shown in Fig. 16. As can be seen, the agreement is very good. The medium transmits the wave above 4.75 GHz. The frequency band of the LH wave propagation is apparent from the dispersion characteristic shown in Fig. 15. This band spans between 4.75 and 5.65 GHz. The frequency band of RH wave propagation is from 5.72 to 11.9 GHz. The bands of the LH and RH propagation nearly

merge, and cannot be distinguished in the transmission characteristic, Fig. 16.

6. Conclusions

This paper summarizes the results of an investigation of left-handed media composed of periodic structures. Each cell of the periodic structure is represented by a segment of the hosting line with a series capacitor and a parallel inductor. These media were treated both as a periodic structure and as a continuous transmission line. The latter is valid when the cell length is much shorter than the wavelength. To validate this concept the LH parallel strips were investigated.

A new left-handed coplanar waveguide was designed, fabricated and measured. The dispersion characteristic calculated by the CST Microwave Studio predicts the pass-bands of the LH and RH modes. The lowest pass-band of the LH wave verified experimentally is about 0.8 GHz in width. A simple equivalent circuit of the left-handed coplanar waveguide was demonstrated and the dispersion characteristic of the first left-handed mode computed using this circuit was compared with the curve computed by the CST Microwave Studio.

A novel bulk metamaterial has been proposed. Its structure incorporates the matrix of the LH transmission lines repeated both horizontally and vertically. These lines consist of parallel strip segments shunted at their centers by inductive pins representing parallel inductors. The segments are separated by short circuited stubs representing series capacitors. The structure behaves as a metamaterial in the frequency band from 4.75 to 5.65 GHz. The transmission and dispersion characteristics of this medium were calculated and measured. They agree very well with each other.

Acknowledgements

References

[1] SMITH, D. R., PADILLA, W. J., VIER, D. C. NEMAT-NASSER, S. C., SCHULTZ, S. Composite medium with simultaneously negative permeability and permittivity. *Phys. Rev. Lett.* 2000, vol. 84, no. p. 4184-4187.

[2] CALOZ, C., ITOH, T. Application of the transmission line theory of left-handed (LH) materials to the realization of a microstrip LH transmission line. In *IEEE-APS International Symposium*. San Antonio, 2002, p. 412-415.

[3] ZIOLKOWSKI, R. W., CHENG, C-Y. Tailoring double negative metamaterial responses to achieve anomalous propagation effects along microstrip transmission lines. In *2003 IEEE MTT-S IMS Digest*. Philadelphia, 2003, p. 203-206.

[4] LIM, S., CALOZ, C., ITOH, T. Metamaterial-based electronically controlled transmission-line structure as a novel leaky-wave antenna with tunable radiation angle and beamwidth. *IEEE Transactions on Microwave Theory and Techiques*. 2005, vol. 53, no. 1, p. 161 to 173.

[5] ANTONIADES, M. A., ELEFTHERIADES, G. V. Compact linear lead/lag metamaterial phase shifters for broadband applications. *IEEE Antennas and Wireless Propagation Letters*. 2003, no. 2, p. 103–106.

[6] LIN, I-H., DEVINCENTIS, M., CALOZ, C., ITOH, T. Arbitrary dual-band components using composite right/left-handed transmission lines. *IEEE Transactions on Microwave Theory and Techniques*. 2004, vol. 52, no. 4, p. 1142–1149.

[7] PENDRY, J. B. Negative refraction makes a perfect lens. *Physical Review Letters*. 2000, vol. 85, no. 18, p. 3966–3969.

[8] ALU, A., ENGHETA, N. Guided modes in a waveguide filled with a pair of single-negative (SNG), double-negative (DNG), and/or double-positive (DPS) layers. *IEEE Transactions on Microwave Theory and Techniques*. 2004, vol. 52, no. 1, p. 199-210.

[9] SANADA, A., CALOZ, C., ITOH, T. Novel zeroth-order resonance in composite right/lefthanded transmission line resonators. In *Proc. Asia-Pacific Microwave Conference*. Seoul (Korea), 2003, p. 1588 to 1592.

[10] ERENTOK, A., LULJAK, P., ZIOLKOWSKI, R. W. Antenna performance near a volumetric metamaterial realization of an artificial magnetic conductor. *IEEE Transactions on Antennas and Propagation*. 2005, vol. 53, no. 1, p. 160–172.

[11] GRBIC, A., ELEFTHERIADES, G. V. Leaky CPW-based slot antenna arrays for millimeter-wave application. *IEEE Trans. On Antennas Propagation*. 2002, vol. 50, no. 11, p. 1494-1504.

[12] SANADA, A., MURAKAMI, K., ASO, S., KUBO, H., AWAI, I. A via-free microstrip left-handed transmission line. In *2004 IEEE MTT-S IMS Digest*. Fort Worth, 2004, p. 301-304.

[13] FALCONE, F., MARTÍN, F., BONACHE, J., MARQUÉS, R., LOPETEGI, T., SOROLA, M. Left handed coplanar waveguide band pass filters based on bi-layer split ring resonators. *Microwave and Wireless Components Letters*. 2004, vol. 14, no. 1, p. 10-12.

[14] COLIN, R. E. *Field Theory of Guided Waves*, 2nd ed. Piscataway: IEEE Press, 1991.

[15] COLIN, R. E. *Foundations for Microwave Engineering*, 2nd ed.. Piscataway: IEEE Press, 2001.

[16] SMITH, D. R., VIER, D. C., KROLL, N., SCHULTZ, S. Direct calculation of permeability and permittivity for a left-handed metamaterial. *Applied Physics Letters*. 2000, vol. 77, no. 14, p. 2246 to 2248.

[17] GHIONE, G., NALDI, C. U. Coplanar waveguides for MMIC applications: effect of upper shielding, conductor backing, finite-extent ground planes, and line-to-line coupling. *IEEE Transactions on Microwave Theory and Techniques*. 1987, vol. 35, p. 260-267.

[18] MAO, S-G., WU, M-S. Equivalent circuit modelling of symmetric composite right/lefthanded coplanar waveguides. In 2005 *IEEE MTT-S IMS Digest*. Long Beach, 2005, paper TH4F-4.

[19] MAO, S.-G., CHEN, S.-L., HUANG, C.-W. Effective electromagnetic parameters of novel distributed left-handed microstrip lines. *IEEE Transactions on Microwave Theory and Techniques*. 2005, vol. 53, no. 4, p. 1515–1521.

[20] TERMAN, F. E. *Radio Engineers' Handbook*, McGraw/Hill, 1945

About Authors...

Jan MACHÁČ graduated in radioelectronics from the Faculty of Electrical Engineering, Czech Technical University in Prague (CTU FEE) in 1977. He was awarded a CSc. (Ph.D. equivalent) degree from the Institute of Radio Engineering and Electronics, Academy of Sciences of the Czech Republic. Since 1984 he has been employed at CTU FEE, where he became an associate professor in 1991 and was awarded the Dr.Sc. (Doctor of Science) degree in 1996. His main research interests are investigation of planar passive elements and subsystems, antennas and periodic structures used in millimeter wave engineering and field theory. Jan Macháč is the author or co-author of more than 130 scientific papers in journals and conference proceedings, and several textbooks. He is a Senior Member of the IEEE. He was a member of the Technical Program Committee of the European Microwave Conference in 1995-1997 and Secretary of this Conference in 1996. He was a member of the TPC of the 2004 URSI International Symposium on Electromagnetic Theory. He is a reviewer of IEEE MTT, Electronics Letters and IEE Proc. Microwaves, Antennas & Propagation, and reviews papers for EuMC.

Martin HUDLIČKA graduated in radioelectronics from the Faculty of Electrical Engineering, Czech Technical University in Prague (CTU FEE) in 2004. At present, he is a Ph.D. student in the Department of Electromagnetic Field CTU FEE in Prague. His main area of interest is propagation of electromagnetic waves in periodic structures, especially metamaterials. He is a Student Member of the IEEE.

Pavel BUCHAR graduated in radioelectronics from the Faculty of Electrical Engineering, Czech Technical University in Prague (CTU FEE) in 2004. At present, he is a Ph.D. student in the Department of Electromagnetic Field CTU FEE in Prague. His main areas of interest are the use of nanostructures in electronics and propagation of electromagnetic waves in periodic structures.

Ján ZEHENTNER graduated from the CTU FEE in 1962, and was awarded a CSc. (Ph.D. equivalent) degree from the Czechoslovak Academy of Sciences, Prague, Czech Republic, in 1972, in radioelectronics engineering, and a Dr.Sc. degree in radioelectronics from CTU FEE, in 1991. He has been with the Faculty of Electrical Engineering, CTU, as an Assistant Professor (1963-1979), Associate Professor (1980-1993), and since 1994 as a Professor of radioelectronics. He has worked on nonlinear effects in optics, passive microstrip circuits, and wideband tunable and stabilized microwave oscillators. His research interests are mainly in the area of planar microwave and millimeter wave circuits, modeling of devices and field theory. Ján Zehentner is the author or co-author of more than 150 scientific papers in journals and conference proceedings and several textbooks. He is a Senior Member of the IEEE. He was the Chairman of the 26th European Microwave Conference. He is a member of the IEEE MTT-S IMS Technical Program Committee, member of the International Program and Steering Committee of the Electromagnetic Fields and Materials Conference, International Symposium on Signals, Systems, and Electronics, member of the IEEE MTT-S Ad Com Membership Services Committee-Region 8 Chapters Coordinator, Head of the Professional Group Microwave Technique of the Czech Electrical Society. He is a member of the Editorial Board of the IEEE Transactions on MTT, Journal of Electrical Engineering and reviewer of Radio Science, EuMC.

Contents Continued from Front Cover